

Supplementary Materials for

Conjugated polymers optically regulate the fate of endothelial colony-forming cells

F. Lodola*, V. Rosti, G. Tullii, A. Desii, L. Tapella, P. Catarsi, D. Lim, F. Moccia, M. R. Antognazza*

*Corresponding author. Email: francesco.lodola@iit.it (F.L.); mariarosa.antognazza@iit.it (M.R.A.)

Published 27 September 2019, *Sci. Adv.* **5**, eaav4620 (2019)

DOI: 10.1126/sciadv.aav4620

This PDF file includes:

Fig. S1. Local and global evaluation of the extracellular bath temperature.

Fig. S2. TRPV1 is endogenously expressed in ECFCs, and it is efficiently activated by polymer photostimulation.

Fig. S3. Current clamp measurements in HEK-293 cells.

Fig. S4. Pharmacological study on ECFCs seeded on polymer substrates in the dark—Evaluation of effect on tubulogenesis.

Fig. S5. Polymer photostability.

Fig. S6. p65 NF- κ B nuclear translocation is unaltered in ECFCs seeded on glass subjected to light-induced photostimulation.

Fig. S7. mRNA levels of proangiogenic genes downstream of NF- κ B signaling.

Table S1. List of oligonucleotide primers used for real-time PCR.

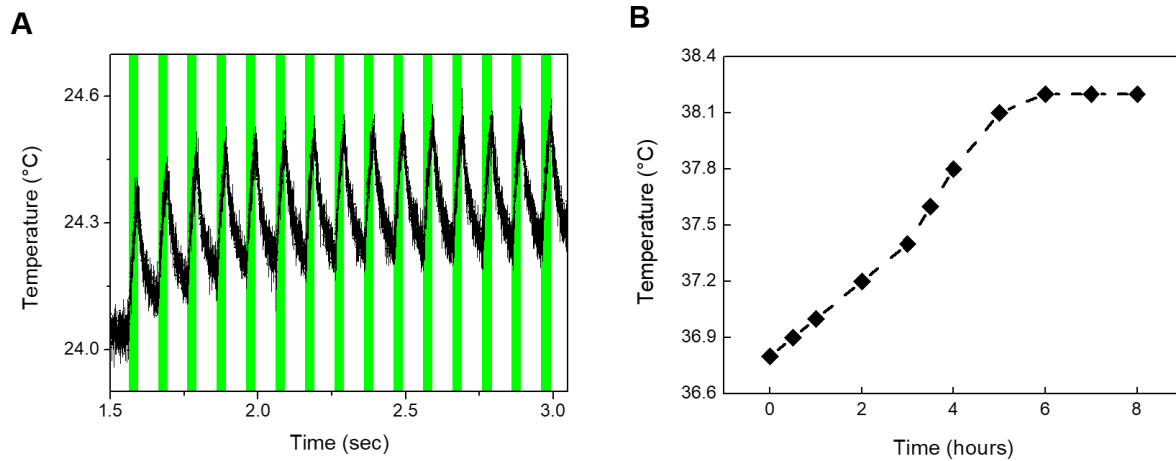


Fig. S1. Local and global evaluation of the extracellular bath temperature. (A) Local temperature variation upon long-term photoexcitation protocol (525 nm, 30 ms light/70 ms dark, 40 mW/cm²; light pulses are represented by green shaded areas) is measured by the method of the calibrated pipette. Due to spatial resolution of the technique, the observed temperature increase should be considered as an average value within the volume of the cylinder defined by the light spot size (base) and about 1 μm height (precision in the positioning of the microelectrode). The measurement shows that heat is efficiently dissipated within the bath and the basal temperature is almost completely recovered during the dark period of 70 ms. (B) Global temperature variation in the bath is measured by a thermocouple inserted in the cell medium, during the long-term polymer excitation protocol (black symbols). The dashed line is a guide to the eye. Temporal and spatial resolution of the thermocouple (> 1s, ~1cm) does not allow to follow fast dynamics of the stimulation protocol, nor to measure heating effects in close proximity of the polymer surface. However, it provides a reliable estimation of the basal temperature increase in the same incubating conditions used for the proliferation and tubulogenesis assays. The discrepancy between the two methods in the evaluation of the temperature increase measured at the equilibrium condition (about 0.5°C and about 1°C, respectively) can be explained by the fact that the measurement is carried out in open environment and at room temperature in the first case, and in a closed environment, within the incubator, in the second case.

Electrophysiological characterization

We employed the patch clamp technique in whole-cell configuration to check the expression of TRPV1 channel in ECFCs and to evaluate the effect of polymer photoexcitation on cell membrane resting potential as well as on channel activation. In this case, the light source was provided by a LED diodes system (Lumencor Spectra X) fibre-coupled to the fluorescence port of the microscope; the illuminated spot on the sample has an area of 0.23 mm^2 . A combination of four different LEDs was employed, providing a broad-band optical emission spectrum, fairly matching the P3HT optical absorption spectrum. The photoexcitation density was measured by a calibrated integrating sphere at 540 nm, at the output of the microscope objective, and it has a value of 344 mW/mm^2 . It is important to notice that, due to the high absorbance of the P3HT active layer, as well as to optical losses due to the petri-dish and the glass substrate, the actual optical density reaching the cell culture is reduced to 87 mW/mm^2 . Acute optical excitation protocol, at variance with the protocol used to enhance cells proliferation and tubulogenesis, consisted in 1 minute-long experimental runs, composed by a 100 ms-long light pulse and 900 ms dark, repeated for 40 times (**fig. S2A** and **S2B**).

Figure S2C reports the variation of the cell membrane potential, as measured in current clamp configuration at $I = 0$, in P3HT-coated and control glass substrates, upon photoexcitation (represented as shaded yellow area) and in dark conditions (**fig. S2C** and **fig. S2D**, respectively). Since, in agreement with previous works (13, 33), no significant variation in the resting membrane potential values before illumination onset was observed in the two conditions, data have been reported as relative variation of the membrane potential, in all cases. Polymer photoexcitation (red solid line) induces a fast depolarization with average amplitude of $4.9 \pm 0.4 \text{ mV}$ (mean \pm SE, $n = 25$). Conversely, illumination of ECFCs cultured on top of visible-transparent, glass substrates (black solid line) does not lead to significant changes in the membrane potential, thus ruling out possible activation of endogenously expressed light-absorbing proteins and indicating the active role played by the polymer in the photo-transduction process (**fig. S2C**). Control measurements in dark conditions further confirm that membrane depolarization originates from the combined action of visible light illumination and polymer absorption (**fig. S2D**).

Recently, we investigated the effect of P3HT photoexcitation on a simplified secondary line cell model, namely on Human Embryonic Kidney cells (HEK-293) (13) as well as on HEK-293 transfected with the Vanilloid Transient Receptor Potential 1 (TRPV1) channel (HEK-293T) (33). The comparison of the present data with both these two cases is instructive. Representative data of the cell membrane potential variation upon polymer photoexcitation in HEK-293 cells are shown in **fig. S3**. Briefly, we observed that in HEK-293 cells the optical excitation of the polymer thin film

leads to an initial, early-activated depolarization, partially overlapping with a longer-activated hyperpolarization (**fig. S3A**). The polarity reversal in the cell membrane potential variation usually occurs over an average temporal scale of few tens of milliseconds (**fig. S3B**). Both these effects have been interpreted on the base of photo-thermal phenomena, and in more detail, they are due to a variation of the membrane capacitance, giving rise to the depolarization signal, and of the Nernst potential, giving rise to the membrane hyperpolarization. Interestingly, a recent work by the Prof. Shoham's group has further explained the thermally-activated depolarization and related capacitance increase as due to an intramembrane thermal-mechanical effect, wherein the phospholipid bilayer undergoes axial narrowing and lateral expansion (36).

HEK-293T cells, endowed with TRPV1 channel, show a different behaviour. In this case, the initial depolarization is partially overlapped with a much stronger, longer activating positive shift in membrane potential, which also completely overwhelms the previously observed hyperpolarization (**fig. S3C**). This behaviour has been unambiguously attributed to the activation of the TRPV1 channels. When the TRPV1 channel activity is inhibited by selective pharmacological agents, the depolarization and hyperpolarization signals are visible, with similar dynamics to those observed in non-transfected cells (13, 33).

Herein, we consider ECFCs, which represent a more complex and therapeutically significant model. In presence of polymer photoexcitation, bioelectrical dynamics combining features similar to those previously evidenced in HEK-293 and HEK-293T cells is evidenced (**fig. S2C**). In fact, P3HT photoexcitation determines the rise of a depolarization signal, which however is neither increasing for the whole duration of the light stimulus, as observed in HEK-293T cells, nor turning into a hyperpolarization signal during the 100 ms-long light stimuli, as observed in non-transfected HEK cells. Conversely, an exponential decrease of the depolarization signal is clearly recognizable, which reaches a plateau during the light excitation. This, in analogy with HEK-293T cells endowed with TRPV1 channels, suggests the involvement of TRPV1 activation also in the present case. In order to verify our working hypothesis, we treated the cell culture with a TRPV1 selective blocker (Capsazepine, CPZ, 10 μ M, **fig. S2E**), a TRPV general blocker (Ruthenium Red, RR 10 μ M, **fig. S2F**), and RN-1734 20 μ M, a selective antagonist of a different temperature-sensitive channel, TRPV4, which is endogenously expressed in ECFCs (34) (**fig. S2G**). Experimental curves have been obtained by averaging data over a statistical ensemble of isolated cells. Importantly, all individual datasets have been acquired on the very same cell, before and after the pharmacology treatment ($n = 8$, $n = 10$ and $n = 7$, for RR, CPZ and RN-1734, respectively). In the presence of either CPZ (**fig. S2E**) or RR (**fig. S2F**), light excitation induces a weaker depolarization that rapidly

drops to negative values, -0.25 mV and -0.75 mV, respectively, and the contribution of the underlying hyperpolarizing effect to the overall signal becomes predominant. This unambiguously indicates the involvement of TRPV1 channel in the observed, longer-activated depolarization signal. Conversely, the TRPV4 specific blocker does not induce any statistically significant effect (**fig. S2G**).

Based both on our previous investigation of HEK-293 cells transfected with TRPV1 and channel activation characterization, showing similar build-up, exponential-like formation dynamics (compatible with a thermal activation), and on experimental evidences provided by pharmacology experiments, we infer that polymer photoexcitation leads to sizable opening of TRPV1 channels. Overall, the observed variation of the cell membrane potential induced by polymer photoexcitation is composed by three overlapping contributions: (i) a fast-activated depolarization of thermal origin, possibly due to a conformational change of the cell membrane and to the related membrane capacitance increase; (ii) a longer-time activation of the depolarizing current due to progressive opening of TRPV1 channels, which in absence of specific antagonist agents gives rise to a sustained depolarization signal; (iii) cell membrane hyperpolarization characterized by longer build-up dynamics, which however becomes predominant only upon administration of TRPV1 blocking agents.

At first approximation, the curve obtained as the difference between the cell membrane potential variation in presence and in absence of CPZ provides a rough way to isolate the sole contribution of TRPV1 channels activation to the depolarization current, at least during the first few tens milliseconds after photoexcitation (where the contribution of the hyperpolarizing signal is expected instead to be negligible). The as obtained curve is characterized by an exponential growth temporal profile, reaching its maximum value within the first few tens milliseconds (**fig. S2H**). Thus, pulses of few tens of ms, at the considered photoexcitation density, are expected to sizably activate TRPV1 channels and to keep the cell membrane continuously depolarized.

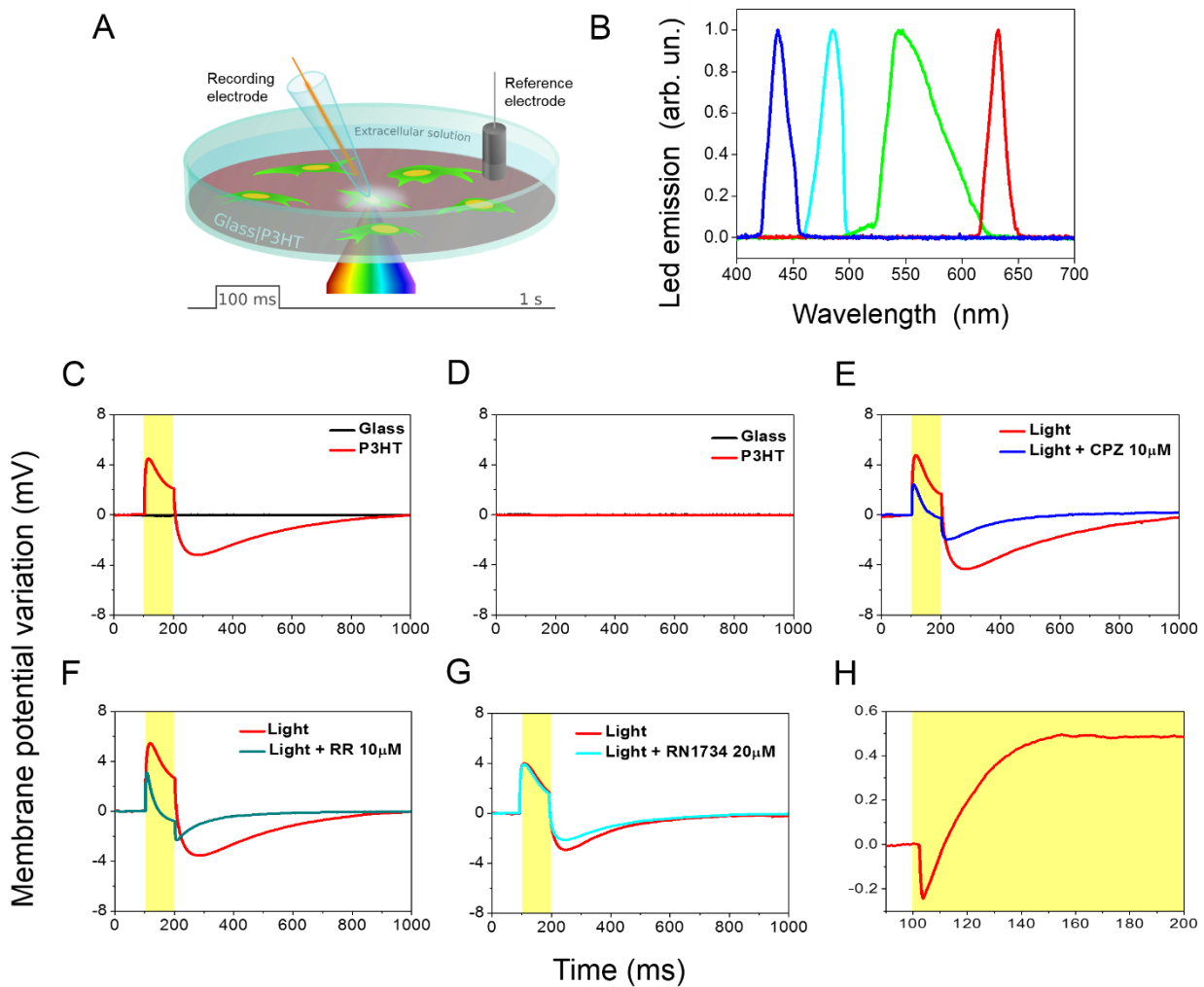


Fig. S2. TRPV1 is endogenously expressed in ECFCs, and it is efficiently activated by polymer photostimulation. (A, B) Experimental set-up and emission spectra of LED sources employed for acute polymer excitation. (C) Cell membrane potential variation upon light excitation, represented by the yellow-shaded area, recorded in cells seeded on polymer thin films (red solid lines) and on control glass substrates (black solid lines). Data have been averaged over a statistical ensemble of 25 cells. (D) Same as in (A), but in dark conditions. $n = 25$. (E, F, G) Membrane potential variation recorded in cells plated on polymer substrates and subjected to polymer photoexcitation, upon administration of selective TRPV1 antagonist agent CPZ ($n = 10$), generic TRPV channel inhibitor RR ($n = 8$) and specific TRPV4 inhibitor RN-1734 ($n = 7$). (H) Membrane potential variation ascribed to TRPV1 channels activation obtained as the difference between representative traces of the cell membrane potential variation in presence and in absence of CPZ.

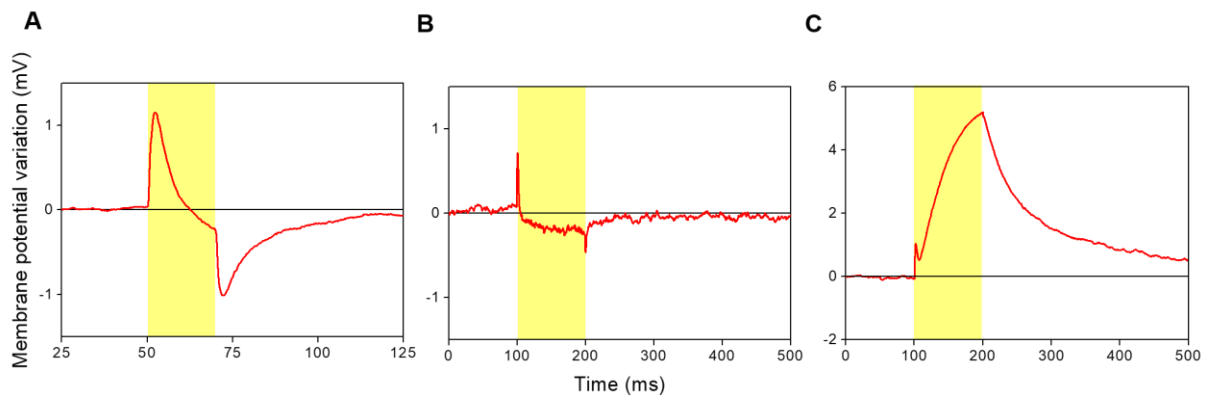


Fig. S3. Current clamp measurements in HEK-293 cells. HEK-293 and HEK-293 transfected with TRPV1 were seeded on P3HT polymer substrates and subjected to optical stimulation. Experimental conditions are fully comparable to the ones employed for short-term optical stimulation protocol of ECFCs plated on P3HT polymer thin films, presented in the main paper (experimental set-up; polymer sample thickness and optical absorbance; light source and stimuli duration; photoexcitation density). **(A, B)** Current clamp ($I = 0$) measurements in non-transfected HEK-293 cells, subjected to 20 ms (A) and 100 ms (B) light pulses. **(C)** Current clamp ($I = 0$) measurements in HEK-293 cells transfected with TRPV1, subjected to 100 ms light pulses.

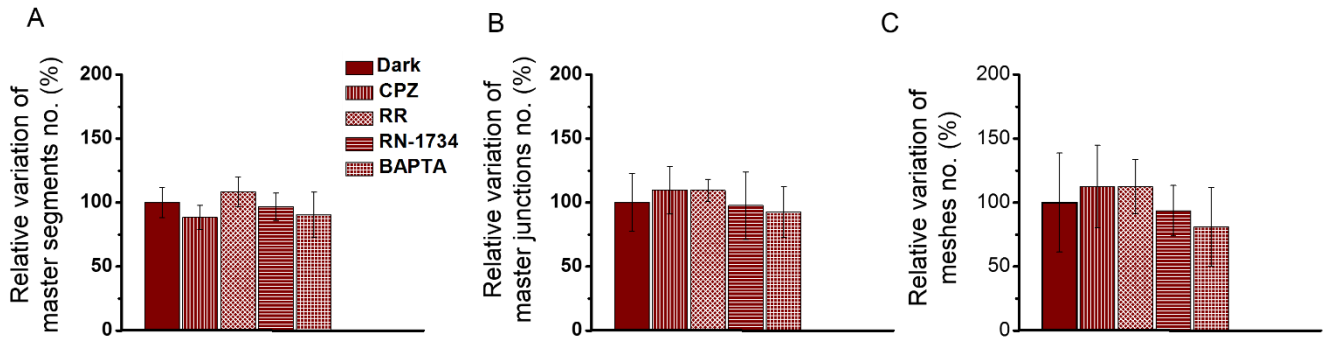


Fig. S4. Pharmacological study on ECFCs seeded on polymer substrates in the dark— Evaluation of effect on tubulogenesis. Relative variation of number of master segments (A), master junctions (B) and meshes (C) of ECFCs kept in dark conditions and seeded on P3HT in absence (Control, CTRL) and presence of 10 μ M Capsazepine (CPZ), 10 μ M Ruthenium Red (RR), 20 μ M RN-1734 (RN-1734) and 30 μ M BAPTA-AM (BAPTA). The results are represented as the mean+SEM of three different experiments conducted on cells harvested from three different donors. The significance of differences was evaluated with one-way analysis of variance (ANOVA) coupled with Dunnett post-hoc test. No statistically significant variation was found.

Polymer photostability assay

The stability of polymer thin films exposed to cell culturing media, to incubating temperature and humidity conditions, and to prolonged optical excitation was assessed by optical absorption, photoluminescence, and Raman spectra measurements. The same experimental protocol used for cell tubulogenesis assays, in terms of photoexcitation density, pulses frequency and overall exposure duration, was employed. Samples exposed to light were compared to samples incubated in dark and to as-prepared samples, before incubation. Optical absorption spectra (**fig. S5A**) do not show significant differences among the considered conditions, thus excluding irreversible degradation effects. Resonant Raman spectra (**fig. S5B**) display the 1350-1550 cm^{-1} spectral range, known to be the active Raman region sensitive to π -electron delocalization (i.e., the conjugation length) of the P3HT chain. The two main peaks at 1378 cm^{-1} and at 1445 cm^{-1} , assigned to C-C stretching and in phase C=C/C-C stretching/shrinking of the aromatic thiophene ring, do not show sizable shift or broadening in the considered conditions, thus corroborating the absence of relevant structural degradation effects. Photoluminescence spectra (**fig. S5C**) are instead heavily affected by exposure to culturing media, and even more by exposure to light, showing a sizable suppression of emission. However, since the absorption does not show relevant changes, the main cause of PL quenching has to be attributed to the enhancement of non-radiative decay. This effect has been previously reported to be partially reversible, upon sample drying and temporary exposure to dark, and in any case it is not expected to seriously hamper the capability of the polymer to generate ROS. Moreover, no clear change in the spectral features of emission are observed, as evidenced by normalized spectra reported in **fig. S5D**. Altogether, the data allow to exclude the occurrence of irreversible degradation phenomena due to exposure to light and subsequent photocatalytic activity.

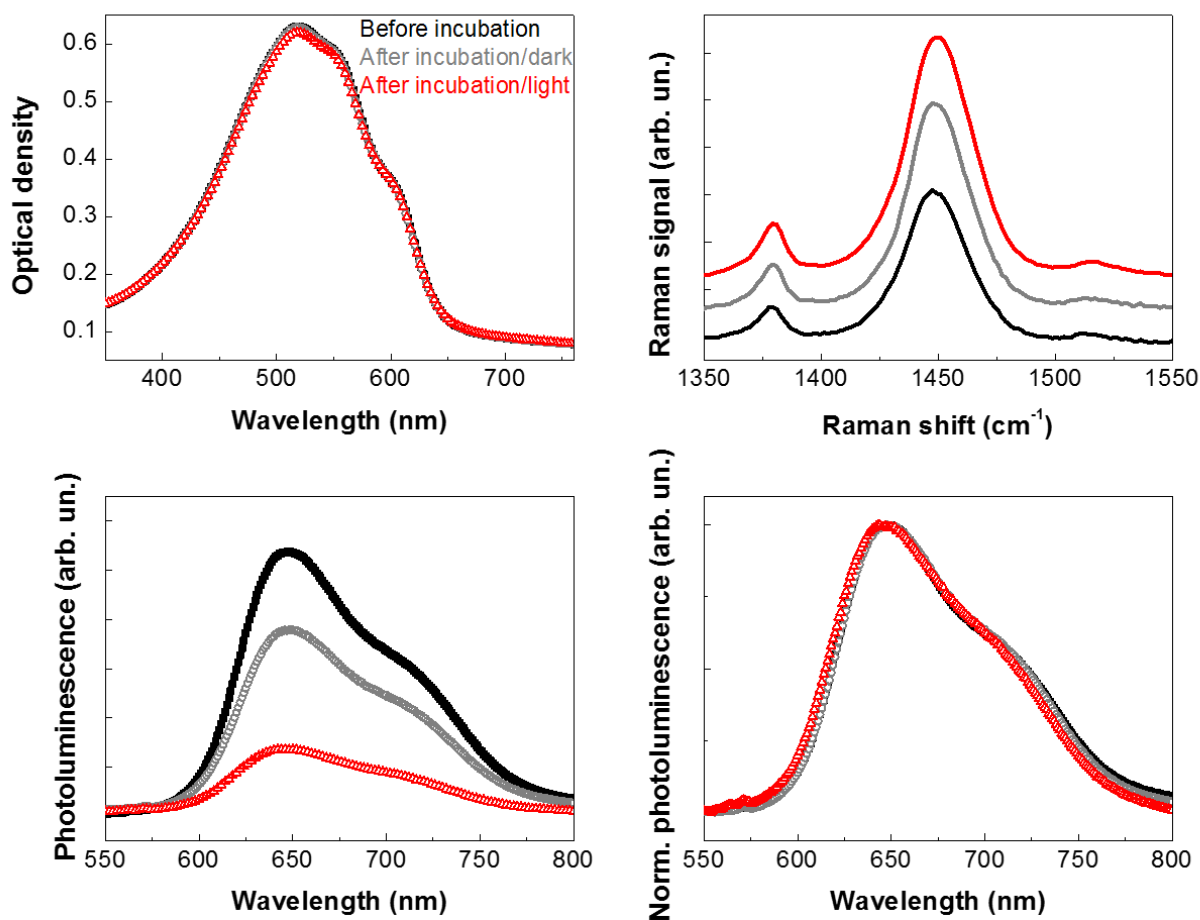


Fig. S5. Polymer photostability. (A) Optical absorption, (B) Raman and (C, D) photoluminescence spectra of P3HT thin films measured immediately after fabrication (black curves) and after exposure to cell growth media in incubating conditions, in dark (grey curves) or subjected to the photostimulation protocol (red curves).

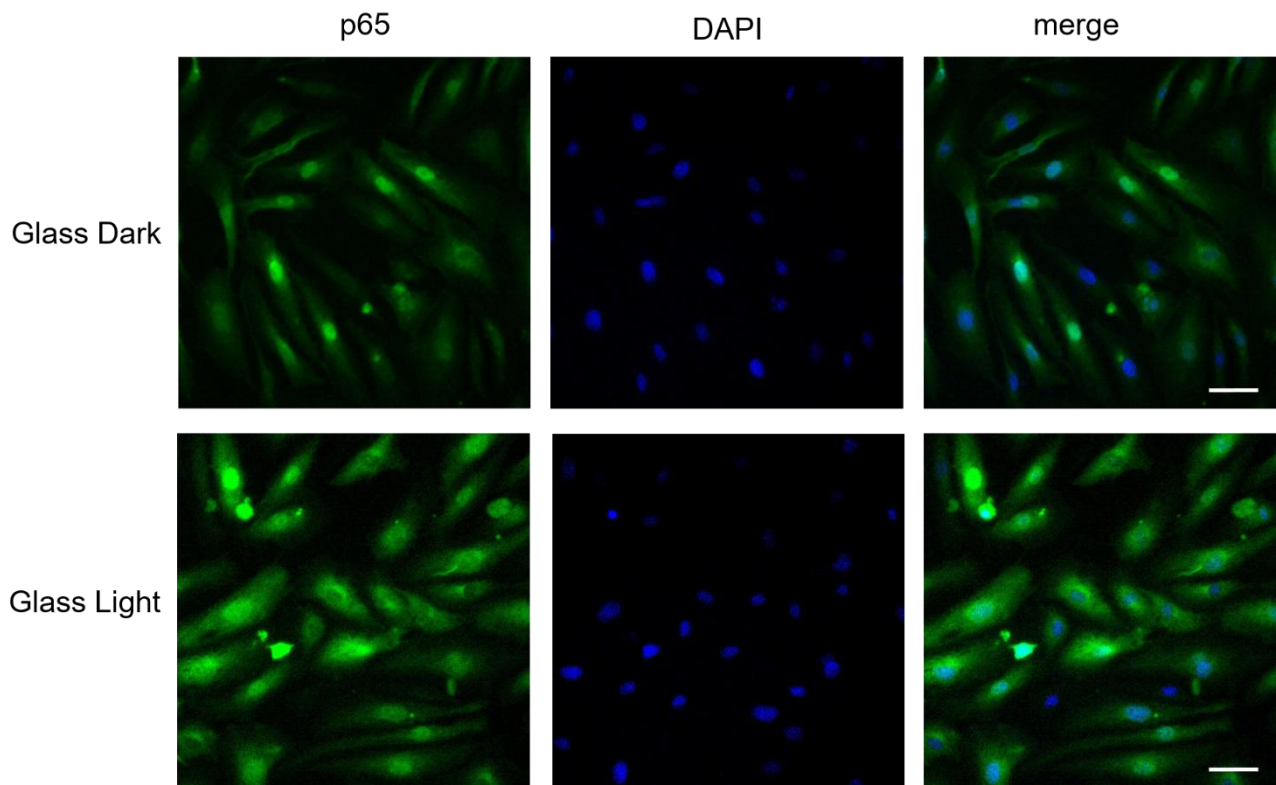


Fig. S6. p65 NF- κ B nuclear translocation is unaltered in ECFCs seeded on glass subjected to light-induced photostimulation. Representative images of immunofluorescence staining showing p65 NF- κ B (green) nuclear translocation in ECFCs seeded on bare glass and subjected to long-term photostimulation and corresponding control samples kept in dark conditions. Cell nuclei were detected by DAPI (blue). Scale bar, 50 μ M.

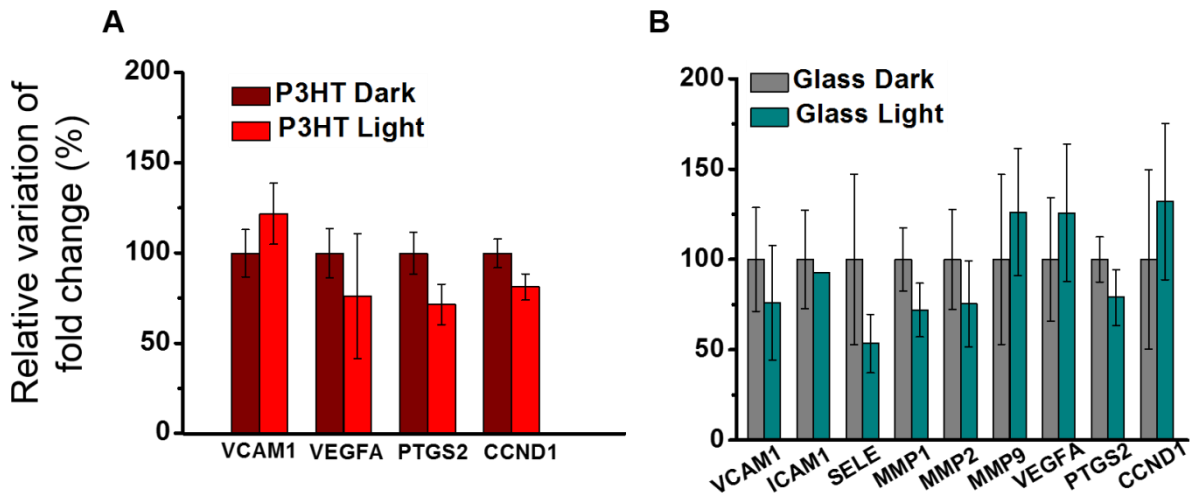


Fig. S7. mRNA levels of proangiogenic genes downstream of NF- κ B signaling. ECFCs grown on P3HT polymer (**A**) or on glass (**B**) were stimulated with light for 8 h, lysed in TRI reagent and processed for real-time PCR. Expression of VCAM1, VEGFA, PTGS2 and CCND1 were not changed upon light exposure in cells grown on P3HT (**A**). Note that none of nine tested genes changed when cells were grown on glass (**B**). Data are expressed as mean \pm SEM from three (VCAM1, VEGFA, PTGS2 and CCND1) or six (ICAM1, SELE, MMP1, MMP2 and MMP9) independent experiments. The significance of differences was evaluated with unpaired Student's t-test.

Table S1. List of oligonucleotide primers used for real-time PCR.

Gene	Accession number	Amplicon length, bp	Forward Reverse	Sequence 5' to 3'
S18	NM_213557	108	Forward Reverse	TGCGAGTACTCAACACCAACA CTGCTTTCCTCAACACCACA
CCND1	NM_053056.2	108	Forward Reverse	TACACCGACA ACTCCATCCG TTCAATGAAATCGTGCGGGG
ICAM1	NM_000201.3	112	Forward Reverse	TGATGGGCAGTCAACAGCTA GCGTAGGGTAAGGTTCTTGC
MMP1	NM_002421.4	111	Forward Reverse	TCATGCTTTTCAACCAGGCC TCATGAGCTGCAACACGATG
MMP2	NM_004530.6	141	Forward Reverse	TGCTCCACCACCTACA ACTT GCAGCTGTCATAGGATGTGC
MMP9	NM_004994.3	120	Forward Reverse	CAGACCTGGGCAGATTCCA CAAAGGCGTCGTC AATCACC
PTGS2	NM_000963.4	149	Forward Reverse	CCCAGGGCTCAAACATGATG TCTAGCCAGAGTTTCACCGT
SELE	NM_000450.2	143	Forward Reverse	TGGCTTCAGTGGACTCAAGT GGTAACCCCTATCACAGCTGA
VCAM1	NM_001078.4	146	Forward Reverse	AAGTTCCTGTTTGCCGAGCT ACCTTCTTGCAGCTTTGTGG
VEGFA	NM_001171623.1	100	Forward Reverse	CTGTCTTGGGTGCATTGGAG GATGATTCTGCCCTCCTCCT